

the other materials was small although the Chitra material had the lowest wear rate. This may be because the colloidal silica particles occupy the space between the larger fillers giving enhanced protection to the polymer matrix.

1. Leinfelder, K. F., *Int. Dent. J.*, 1987, **37**, 152–157.
2. Mair, L. H., Vowles, R. W. and Cunningham, J., *Br. Dent. J.*, 1990, **169**, 355–359.
3. McKinney, J. E. and Wu, W., *J. Dent. Res.*, 1985, **64**, 1326–1331.
4. Mair, L. H., Stolarski, T. A., Vowles, R. W. and Lloyd, C. H., *J. Dent.*, 1996, **24**, 141–148.
5. Lutz, F., Phillips, R. W., Roulet, J. F., Setcos, J. C., *J. Dent. Res.*, 1984, **63**, 914–920.
6. Kusy, R. P. and Leinfelder, K. F., *J. Dent. Res.*, 1977, **56**, 544.
7. Mair, L. H., *J. Dent.*, 1995, **23**, 107–112.
8. Williams, G., Lambrechts, P. and Bream, M. A., *Dent. Mater.*, 1992, **8**, 310–319.
9. Aker, J. R., *J. Am. Dent. Assoc.*, 1992, **150**, 633–635.

ACKNOWLEDGEMENTS. We thank Prof. D. F. Williams, Department of Clinical Engineering, University of Liverpool, UK for providing facilities and Dr S. N. Pal, SCTIMST, India for providing the Chitra samples. V.K.K. is grateful to British Council for funding this work.

Received 11 November 1997; revised accepted 20 January 1998

plutons, has given a U–Pb zircon age of 765 Ma (ref. 2) and K–Ar age of 512 ± 14 Ma (ref. 3).

Kalpatta granite, an elliptical stock (area ca. 50 km^2), trending NNW–SSE, intrudes into the Precambrian crystallines, consisting of hornblende–biotite gneiss and charnockite. Pyroxene granulite, amphibolite and talc–tremolite–actinolite schist are seen as enclaves and bands in the gneiss (Figure 1). The rocks, except granite, have suffered high-grade metamorphism and polyphase deformation resulting in the formation of three generations of folds and a penetrative foliation. The granite pluton, discordant with the host rocks, contains enclaves of gneiss and charnockite near the contact. The overall characters of the pluton suggest that it is post-tectonic.

The granite pluton is massive except for a weak planar fabric near the contact. Surmicaceous⁴, amphibolite and charnockite enclaves of different shapes and sizes are observed along the contact. The absence of enclaves of metasediments within the granite and absence of migmatite zone at the country rock–granite contact preclude the formation of the granite through partial fusion of metasedimentary country rocks. Though the granite appears to be homogeneous, textural and mineralogical variants, ranging from porphyritic to equigranular and

Petrochemistry and petrogenesis of Kalpatta granite, South India

S. N. Kumar*,§, V. Prasannakumar[†] and P. K. R. Nair[†]

*Department of Geology, University College, Thiruvananthapuram 695 034, India

[†]Department of Geology, University of Kerala, Thiruvananthapuram 695 581, India

Kalpatta granite is one among the acid plutons puncturing the Precambrian rocks of Kerala consisting of three dominant phases. The polyphase pluton is a well-differentiated, calc-alkaline, peraluminous, post-orogenic, A-type granite ranging in composition from granite to granodiorite–adamellite. Geochemical discriminant diagrams, mineralogy, and major and trace element chemistry suggest that the variants are products of polyphase late magmatic crystallization.

PRECAMBRIAN rocks of Kerala are intruded by a variety of plutons, ranging in composition from ultrabasic to acidic. Acid igneous activity is manifested by granite intrusives falling within the span of 740 ± 30 Ma and 512 ± 20 Ma (ref. 1). Kalpatta granite, one among such

§For correspondence.

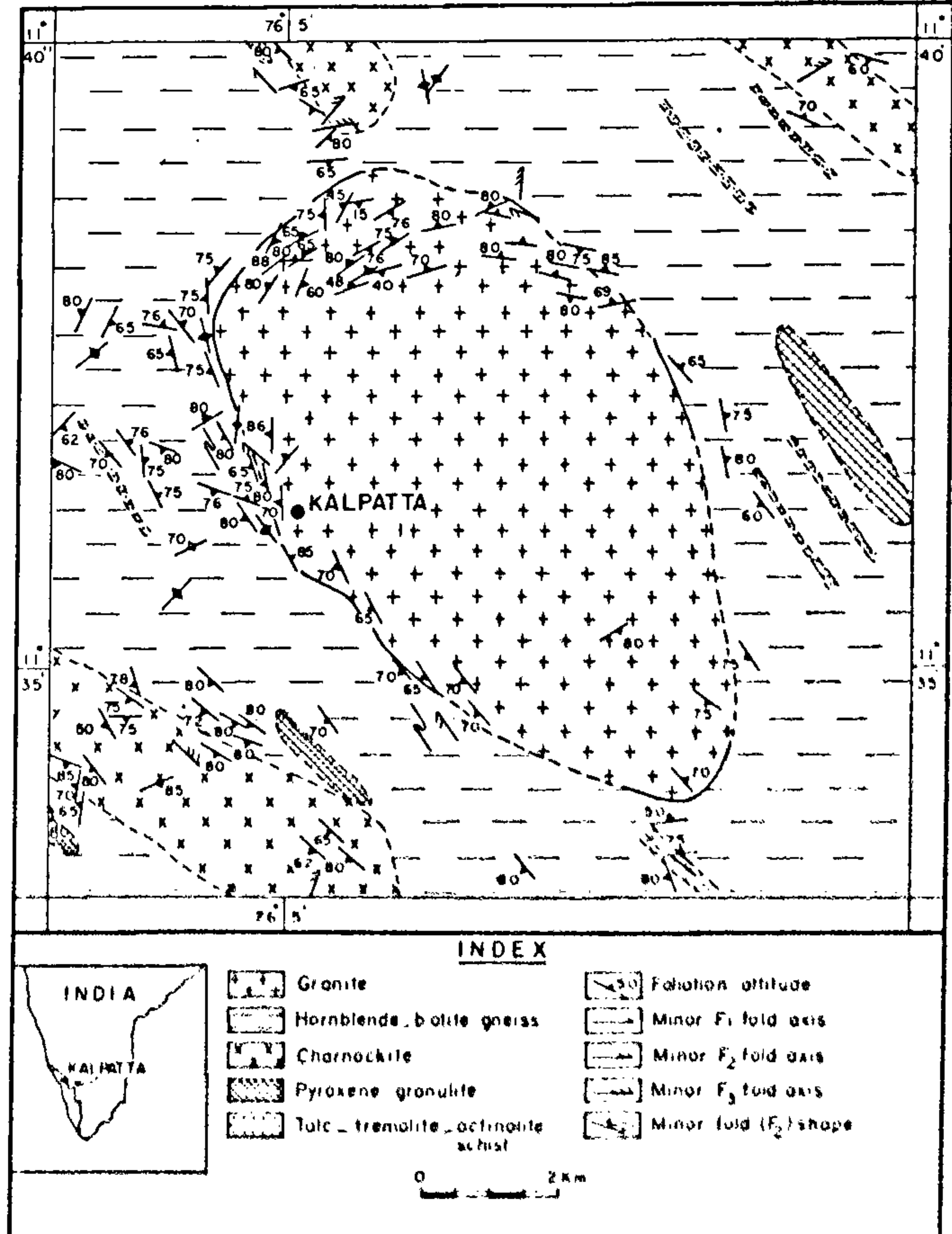


Figure 1. Geological map of the area around Kalpatta

Table 1. Major and trace element compositions – Biotite-rich granite

Sample No.	8-1	12-1	13-5	14	16	24-1	25-1	27-1	28-1	29-1	31-1	32-1	35-1	77
SiO ₂	71.05	71.35	70.94	70.94	71.12	68.33	68.45	71.74	69.30	68.65	70.01	69.48	69.81	71.42
Al ₂ O ₃	14.63	14.21	15.01	15.16	14.44	16.48	16.42	14.20	15.92	16.21	15.65	15.75	15.62	14.28
TiO ₂	0.20	0.21	0.14	0.14	0.40	0.40	0.29	0.38	0.42	0.44	0.37	0.41	0.42	0.42
Fe ₂ O ₃	1.01	1.05	1.21	0.35	0.85	1.04	0.80	0.74	0.94	0.90	1.01	0.94	0.29	0.90
FeO	0.90	1.15	1.35	1.20	1.29	1.21	1.41	1.21	1.30	1.19	1.35	1.46	1.47	1.30
CaO	1.58	1.70	1.73	1.27	1.37	1.38	1.82	1.39	1.95	1.85	1.98	2.01	1.85	1.47
MgO	0.68	0.85	0.69	0.61	0.62	0.71	0.94	0.72	0.93	0.85	0.91	0.92	0.87	0.65
Na ₂ O	4.88	4.85	5.02	5.50	4.72	5.00	4.98	4.65	4.31	5.25	3.89	4.25	4.58	5.06
K ₂ O	3.95	4.10	3.84	4.60	4.05	5.03	4.10	4.21	4.22	3.69	3.71	3.94	4.38	4.32
P ₂ O ₅	0.06	0.03	0.03	0.03	0.04	0.13	0.14	0.01	0.11	0.13	0.05	0.14	0.11	0.03
LOI	0.58	0.30	0.35	0.31	0.46	0.26	0.40	0.42	0.37	0.39	0.53	0.48	0.41	0.35
Total	99.62	99.80	100.31	100.04	99.36	100.24	99.76	99.67	99.77	99.55	99.46	99.64	99.81	100.22
V	3.19	7.73	15.99	12.32	3.24	5.42	5.62	4.98	4.72	5.16	5.72	3.97	3.46	7.85
Cr	41.92	39.35	59.21	14.32	48.51	56.36	59.36	70.00	54.16	65.13	54.00	85.61	56.16	40.15
Ni	2.71	3.81	1.92	1.90	2.62	1.21	1.00	1.32	1.72	1.95	9.45	7.81	1.47	3.27
Co	4.86	7.79	5.73	5.64	4.92	46.16	42.67	5.17	4.62	4.05	4.81	3.61	3.91	6.56
Cu	0.94	1.34	0.85	0.91	0.96	0.91	0.84	0.91	0.98	0.90	1.24	5.68	0.57	1.16
Zn	24.34	30.89	26.33	29.31	26.41	30.51	29.80	32.00	31.42	39.05	35.00	23.41	68.16	32.12
Ga	23.55	25.27	26.51	27.15	24.17	24.17	23.89	24.79	29.16	27.15	24.02	21.97	21.05	26.17
Rb	84.05	101.76	82.33	86.10	105.10	70.12	83.23	66.15	92.45	86.43	84.17	105.15	80.15	91.12
Sr	234.40	250.56	204.16	182.15	260.15	252.17	217.56	231.40	261.08	213.17	192.46	161.26	210.16	185.16
Y	49.83	58.04	47.14	46.95	51.26	56.17	53.94	54.45	41.38	41.13	40.15	38.21	39.81	52.15
Zr	76.36	44.32	81.82	95.45	78.15	95.67	93.81	96.15	105.10	110.40	98.56	207.16	89.15	125.40
Nb	32.83	35.25	26.84	26.71	31.26	28.45	28.25	27.15	29.21	28.71	29.21	31.15	32.76	33.21
Ba	1035.63	1101.80	854.24	925.16	1081.40	1415.62	1353.22	546.50	1315.15	1271.50	1156.10	1185.16	921.15	1215.51
Ta	0.60	0.58	0.22	0.36	0.49	0.42	0.32	0.31	0.37	0.42	0.38	1.28	1.26	0.60
Pb	62.90	56.05	72.39	71.16	65.14	65.16	64.66	62.16	61.56	56.17	67.52	42.16	48.16	58.12
Th	7.98	13.24	6.18	9.90	7.48	5.72	4.12	4.27	4.18	6.08	5.26	9.76	8.96	12.91
U	1.59	1.45	1.75	1.89	1.37	2.67	2.76	2.72	2.11	1.59	1.61	0.91	1.62	1.92
Li	< 10.00	14.00	< 10.00	< 10.00	< 10.00	15.00	< 10.00	11.00	< 10.00	< 10.00	11.00	< 10.00	14.00	16.00

Table 1. (Contd.)

Sample No.	78-1	79	85	87-1	93-1	94	95	98-1	100	103-1	104	106	107-1	108
SiO ₂	68.55	70.31	69.60	69.23	69.31	70.73	70.15	71.72	71.63	72.14	70.04	70.03	69.70	69.88
Al ₂ O ₃	16.31	15.25	15.81	15.99	15.97	15.05	15.35	14.32	14.75	14.05	15.60	15.61	15.77	15.67
TiO ₂	0.38	0.43	0.41	0.33	0.18	0.24	0.47	0.14	Tr	0.23	0.27	0.41	0.33	0.44
Fe ₂ O ₃	1.16	0.92	0.71	0.90	1.14	0.87	0.81	1.01	0.29	0.85	0.67	0.92	1.20	1.01
FeO	1.03	1.10	1.10	1.30	0.62	1.25	1.40	0.85	1.10	1.20	1.30	1.10	1.34	1.32
CaO	1.98	2.10	1.74	1.72	1.85	1.35	1.71	1.92	1.38	1.35	1.40	1.60	1.69	1.57
MgO	0.89	0.90	0.89	0.83	0.84	0.67	0.85	0.93	0.69	0.64	0.71	0.78	0.91	0.81
Na ₂ O	4.78	4.31	5.12	4.86	5.12	4.94	4.10	4.90	4.96	4.88	4.93	4.31	4.45	5.00
K ₂ O	4.51	4.21	4.31	4.66	4.10	4.64	4.48	3.49	4.89	4.46	4.80	4.45	4.22	4.28
P ₂ O ₅	0.14	0.05	0.12	0.11	0.12	0.03	0.02	0.04	0.04	0.03	0.02	0.01	0.11	0.09
LOI	0.29	0.27	0.33	0.43	0.41	0.34	0.26	0.44	0.33	0.25	0.21	0.38	0.37	0.23
Total	100.01	99.85	100.01	100.36	99.66	100.11	99.60	99.76	99.56	100.08	99.85	99.60	99.99	100.30
V	30.12	27.10	39.65	33.73	19.25	4.72	24.41	4.61	4.72	2.56	3.47	3.61	3.48	3.56
Cr	68.10	82.84	72.57	84.96	67.70	72.57	79.15	17.67	41.56	16.69	56.12	17.46	79.16	55.18
Ni	5.64	6.24	8.94	7.14	4.26	4.21	5.94	1.48	4.27	1.43	1.45	4.49	6.14	1.45
Co	1.09	3.00	5.07											

Table 1. (Contd.)

Sample No.	111	112	113	115	116	117	118	119	120	121	132	138-1	142	149-1	Mean
SiO ₂	68.61	71.50	71.18	69.74	70.75	70.81	69.91	70.18	69.75	71.36	71.21	71.50	71.25	71.06	70.34
Al ₂ O ₃	16.35	14.18	14.48	15.74	14.97	14.89	15.58	15.34	15.84	14.35	14.44	14.17	14.40	14.71	15.20
TiO ₂	0.30	0.27	0.31	0.19	0.39	0.32	0.32	Tr	0.22	0.24	0.30	0.29	0.15	0.19	0.30
Fe ₂ O ₃	0.89	0.78	0.91	1.07	0.65	0.67	0.94	0.34	0.63	0.69	0.81	0.65	0.43	0.61	0.82
FeO	0.96	1.39	1.15	1.40	1.32	0.99	1.38	1.71	1.37	1.25	1.32	1.28	1.40	1.39	1.19
CaO	1.71	1.34	1.48	1.47	1.68	1.86	1.79	1.76	1.39	1.58	1.85	1.81	1.80	1.67	1.66
MgO	0.89	0.71	0.85	0.72	0.69	0.84	0.89	0.87	0.67	0.79	0.91	0.98	0.69	0.79	0.80
Na ₂ O	4.45	4.76	4.72	4.78	5.12	4.45	4.71	4.95	5.25	4.35	4.78	4.58	5.10	4.13	4.77
K ₂ O	5.06	4.63	4.09	4.21	4.40	4.29	4.22	4.31	4.45	4.85	4.21	4.08	4.10	4.40	4.31
P ₂ O ₅	0.13	0.02	0.06	0.10	0.09	0.04	0.10	0.04	0.10	0.02	0.03	0.01	0.03	0.05	0.07
LOI	0.41	0.30	0.39	0.33	0.28	0.34	0.31	0.28	0.28	0.27	0.43	0.38	0.34	0.38	0.35
Total	99.66	99.88	99.62	99.75	100.34	99.49	100.15	99.78	99.95	99.75	100.29	99.73	99.69	99.88	99.46
V	2.47	3.28	2.38	3.90	2.78	2.62	3.52	3.56	34.46	4.06	4.49	3.15	8.46	2.32	9.61
Cr	69.47	48.64	16.95	79.21	20.56	56.06	54.17	54.11	77.55	52.16	55.80	47.63	40.71	54.77	54.37
Ni	1.46	2.75	1.35	6.10	1.55	1.27	1.42	3.54	7.20	3.62	2.86	2.44	4.52	2.62	3.51
Co	3.81	3.26	3.30	3.46	4.43	3.96	3.96	5.98	3.55	4.12	3.27	3.15	3.45	2.31	6.00
Cu	0.94	0.74	0.53	0.94	0.66	0.47	0.59	0.94	5.52	1.01	0.30	0.28	4.10	1.00	1.80
Zn	24.92	34.41	54.81	50.16	60.00	61.56	67.01	35.75	49.26	36.44	32.26	25.97	36.10	7.84	40.76
Ga	21.56	23.15	19.92	25.26	17.60	16.85	19.28	24.47	24.19	23.48	22.49	21.25	23.91	23.11	22.79
Rb	93.54	91.12	89.56	81.12	89.45	82.34	83.16	102.76	68.23	136.15	97.55	88.76	89.56	102.06	85.41
Sr	182.55	181.42	187.54	195.15	156.46	194.41	201.46	125.16	272.44	141.46	198.41	201.42	179.50	132.43	198.99
Y	35.11	44.28	35.72	41.51	38.14	39.26	39.57	40.68	41.53	39.13	44.23	44.34	79.41	41.60	42.04
Zr	49.45	121.42	53.61	110.15	61.31	72.15	86.15	71.46	351.57	79.41	94.56	115.86	92.96	133.91	132.34
Nb	30.72	34.68	31.18	25.71	36.74	35.41	34.21	34.00	25.41	36.28	37.67	35.73	38.42	33.06	30.77
Ba	1150.12	1121.45	569.82	861.52	818.57	828.50	939.61	1073.74	1381.60	831.60	1320.61	1019.84	855.10	783.31	1080.32
Ta	0.89	0.62	1.17	0.52	1.43	1.41	1.25	0.50	0.51	0.57	0.58	0.55	0.62	0.35	0.80
Pb	51.42	51.45	50.11	63.16	41.40	47.46	42.41	45.39	62.86	58.32	59.99	52.88	23.46	66.95	52.45
Th	7.26	13.91	8.73	4.39	11.33	9.26	9.76	9.46	4.67	11.37	14.96	14.82	10.16	8.73	8.33
U	1.72	2.47	2.19	1.73	1.84	1.61	1.72	2.65	1.93	2.97	2.23	2.59	1.92	3.85	2.73
Li	10.00	19.00	15.00	17.00	10.00	< 10.00	12.00	20.00	19.00	20.00	10.00	< 10.00	< 10.00	< 10.00	< 10.00

Table 1. (Contd.): Major and trace element composition – Biotite-poor granite

Sample No.	12-2	13-2	13-3	24-2	25-3	28-2	31-2	32-2	98-3	99-2	103-2	138-2	149-2	Mean
SiO ₂	71.50	72.20	69.95	70.92	71.63	70.08	72.02	70.75	71.49	71.75	70.85	71.20	71.94	71.23
Al ₂ O ₃	15.81	15.85	15.91	15.79	15.77	15.55	15.45	15.81	15.90	15.41	15.83	15.74	16.02	15.78
TiO ₂	0.15	0.13	0.17	0.19	0.14	0.21	0.18	0.18	0.20	0.11	0.11	0.17	0.05	0.15
Fe ₂ O ₃	0.31	0.34	0.35	0.34	0.44	0.35	0.27	0.37	0.30	0.19	0.37	0.35	0.29	0.33
FeO	1.01	0.65	1.10	1.10	0.70	0.81	0.47	0.79	0.71	0.81	0.65	0.78	0.79	0.80
CaO	1.14	0.98	1.21	1.45	1.07	0.98	1.01	1.25	1.02	1.19	1.21	1.08	1.01	1.12
MgO	0.34	0.21	0.36	0.41	0.44	0.38	0.35	0.48	0.31	0.39	0.28	0.37	0.34	0.36
Na ₂ O	4.37	4.95	4.95	4.69	4.59	4.41	4.18	4.68	4.84	4.18	4.68	4.78	4.89	4.63
K ₂ O	4.92	4.42	4.35	5.38	5.23	5.38	4.98	4.48	4.59	5.28	5.24	4.17	4.67	4.85
P ₂ O ₅	0.06	0.01	0.10	0.04	0.02	0.09	0.02	0.04	0.06	0.03	0.04	0.04	0.03	0.04
LOI	0.31	0.35	0.38	0.41	0.49	0.41	0.54	0.39	0.29	0.45	0.47	0.34	0.34	0.40
Total	99.92	100.09	98.83	100.72	100.52	98.65	99.47	99.22	99.71	99.79	99.73	99.02	100.40	99.69
V	6.40	8.97	5.40	12.57	7.51	6.12	19.86	3.17	3.59	9.43	1.43	3.75	4.15	7.49
Cr	61.00	57.8												

ferromagnesian-rich to ferromagnesian-poor, can be distinguished. On the basis of field relations, colour, texture and mineralogy three main phases have been identified.

Biotite-rich granite (BRG) is the dominant phase, which shows sharp discordant contacts with the gneiss and is a mesocratic, coarse to fine-grained, equigranular biotite-rich granite. Intercalations of BRG and hornblende-biotite gneiss as well as enclaves of gneiss and amphibolite of different shapes like angular, ellipsoidal, flattened and polygonal, ranging in size from 9 mm to as much as 1.5 m across, are present in the contact zone. Concentration of these enclaves and surmicaceous schlieren near the margin indicates the magmatic origin of granite. Quartz (24.65%), K-feldspar (42.84%), plagioclase (23.92%) and biotite (7.01%) are the major constituents, while zircon, sphene, apatite and magnetite

form the accessories. Among feldspars, K-feldspar is dominant – particularly microcline. Perthite intergrowth is common in microcline, the textural variations being spindle, string and flame types. Perthites, when in contact with plagioclase, develop a rim of albite possibly derived by exsolution from a monoclinic potash-soda feldspar as a consequence of the accompanying submagmatic inversion to non-perthitic triclinic microcline⁵. Two varieties of biotite – one pleochroic from shining pale green to dark green and the other from colourless to yellowish brown – occur as flakes and wisps. Perthite + green biotite assemblage is characteristic of A-type granites⁶, while the two feldspars (perthite and plagioclase) + biotite ± hornblende are common in post-orogenic granites⁷.

Biotite-poor granite (BPG) consists of veins and bands

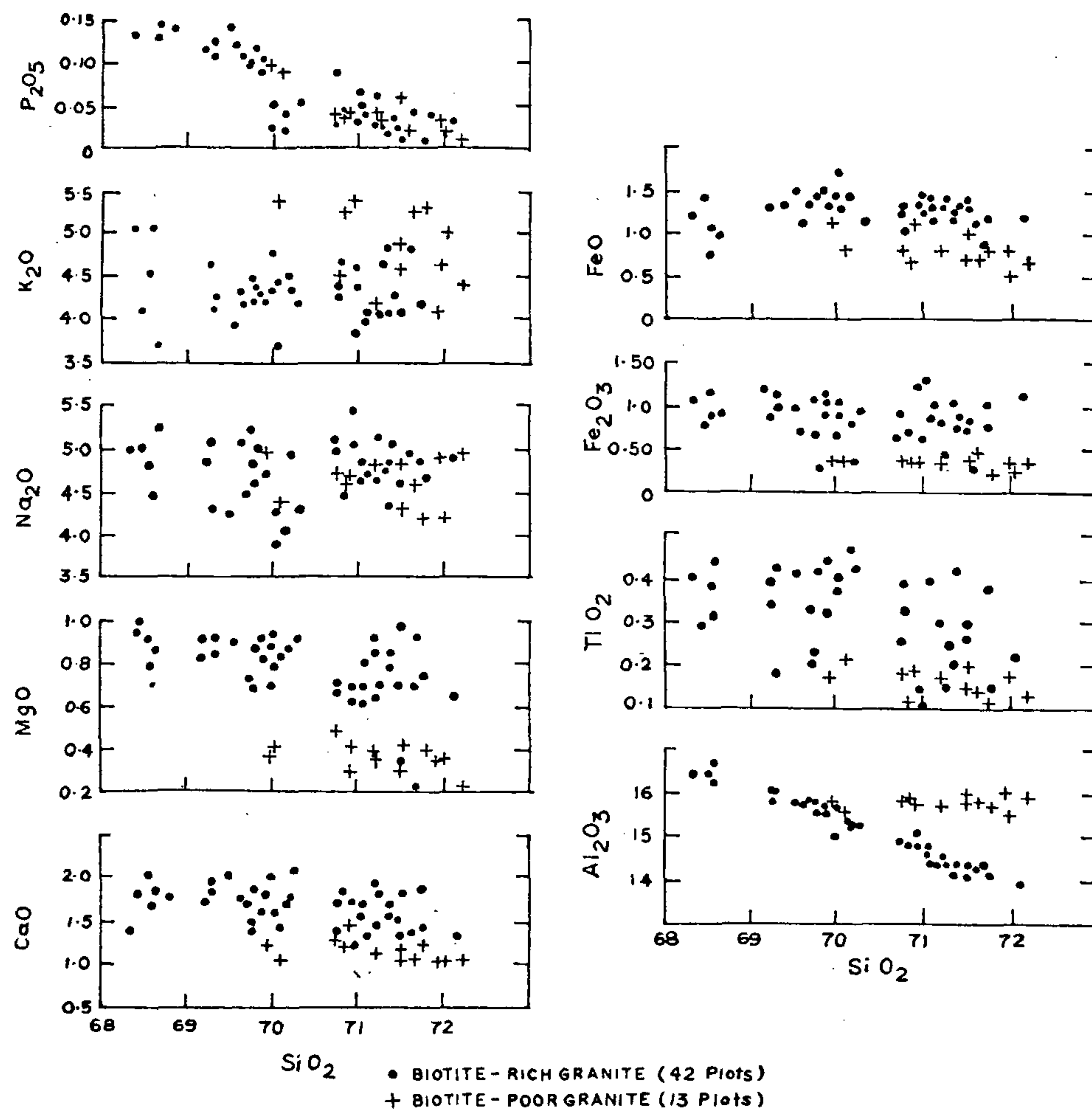
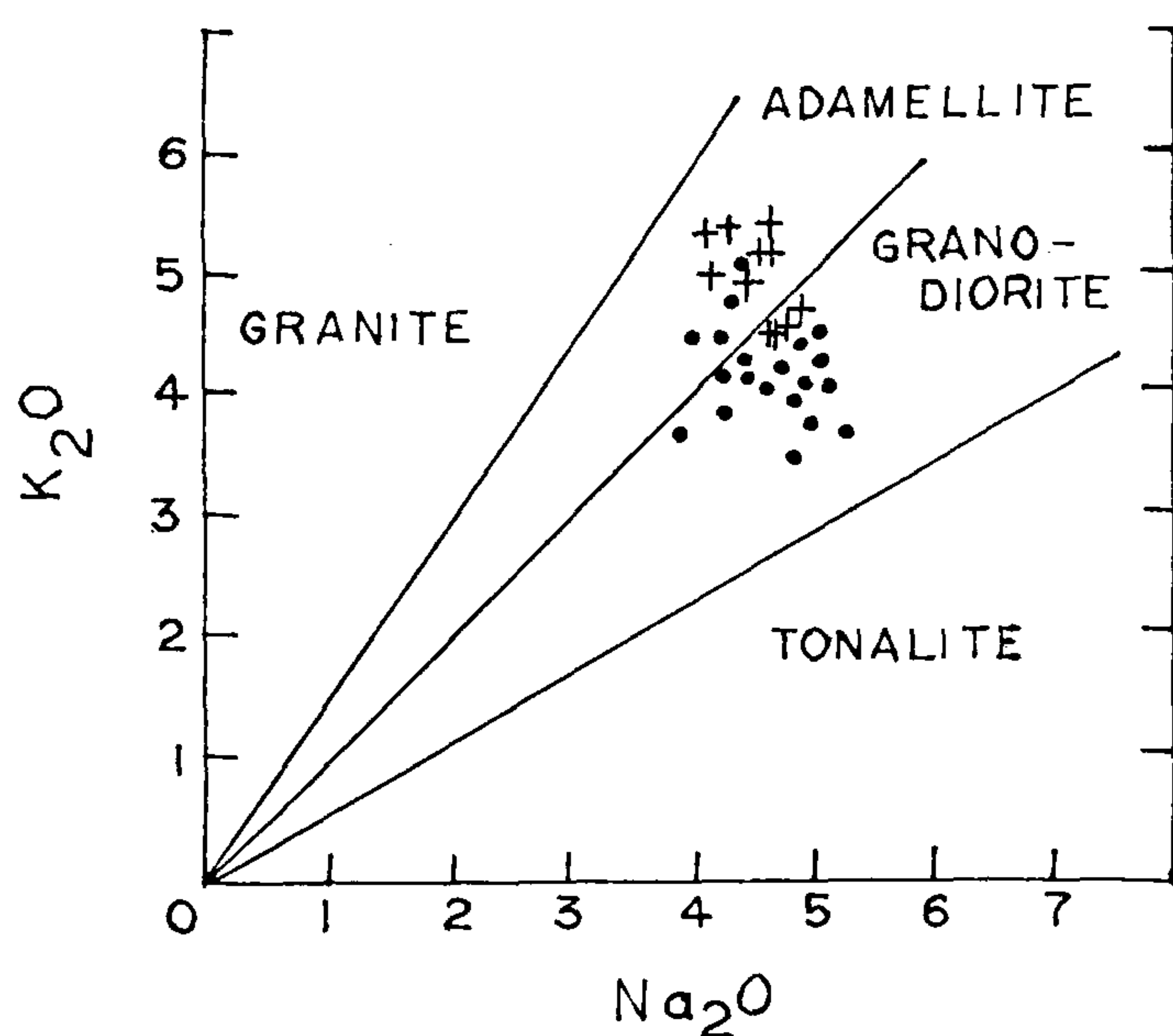
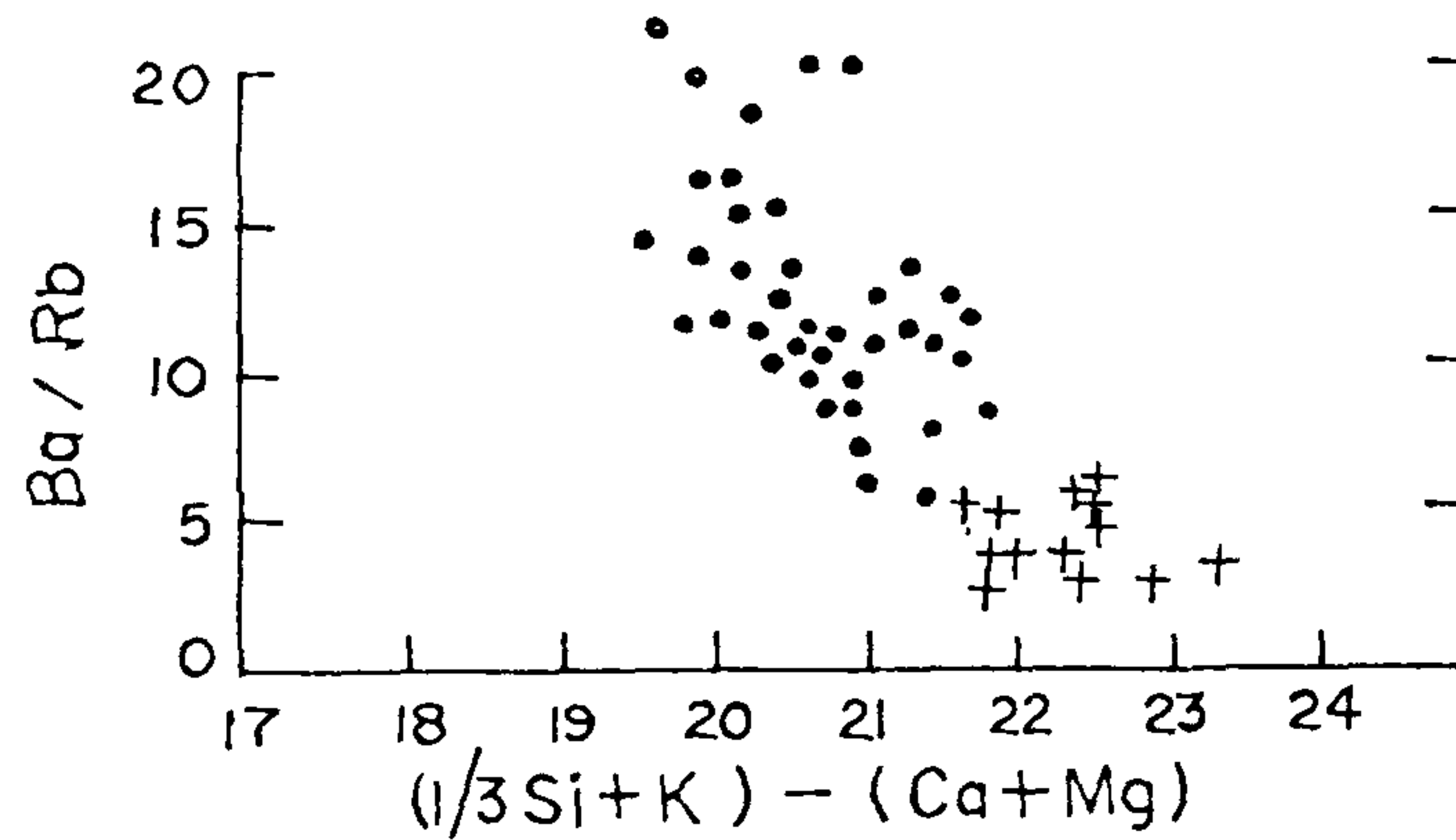
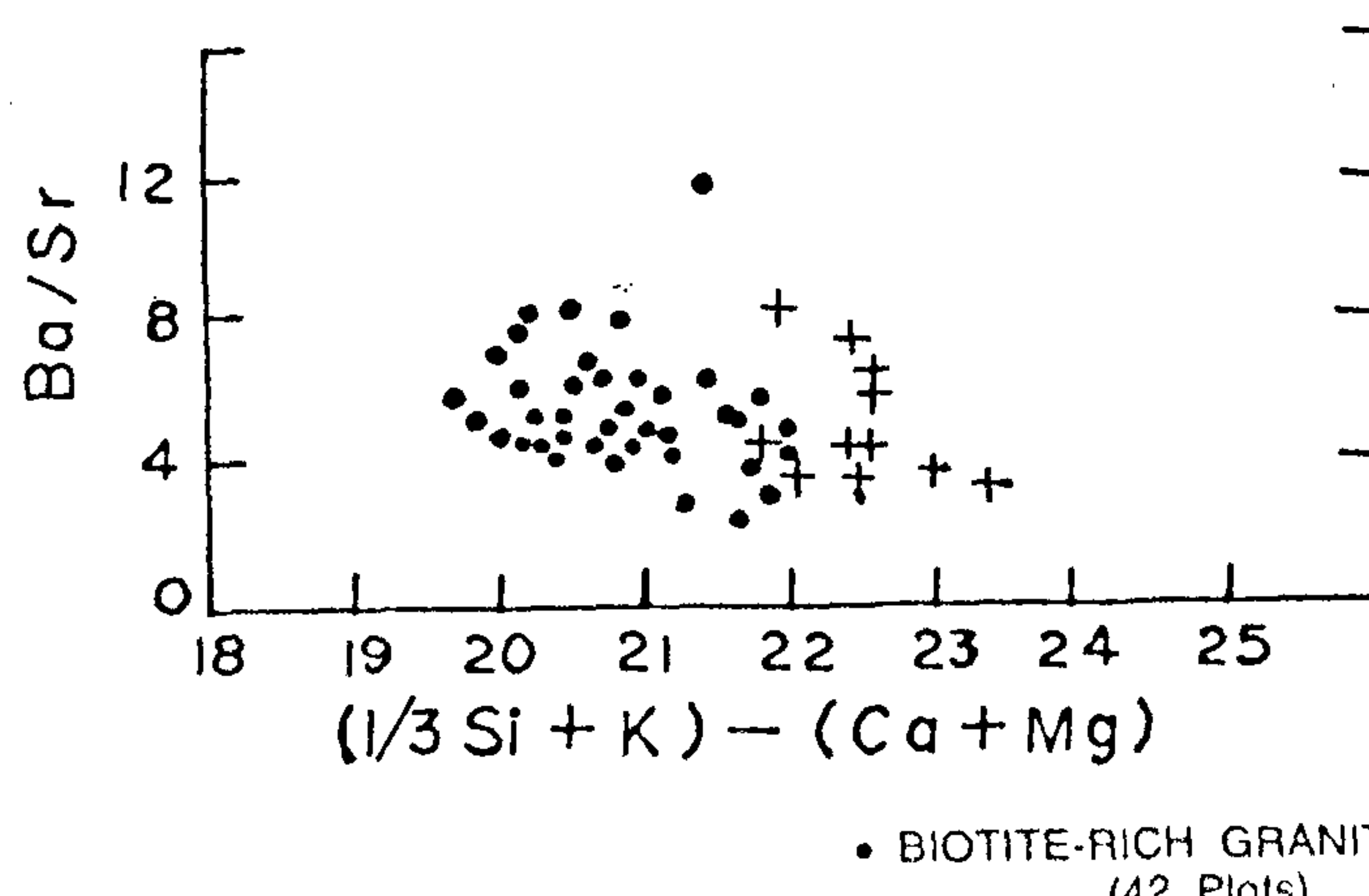


Figure 2. Harker variation diagram for Kalpatta granite.

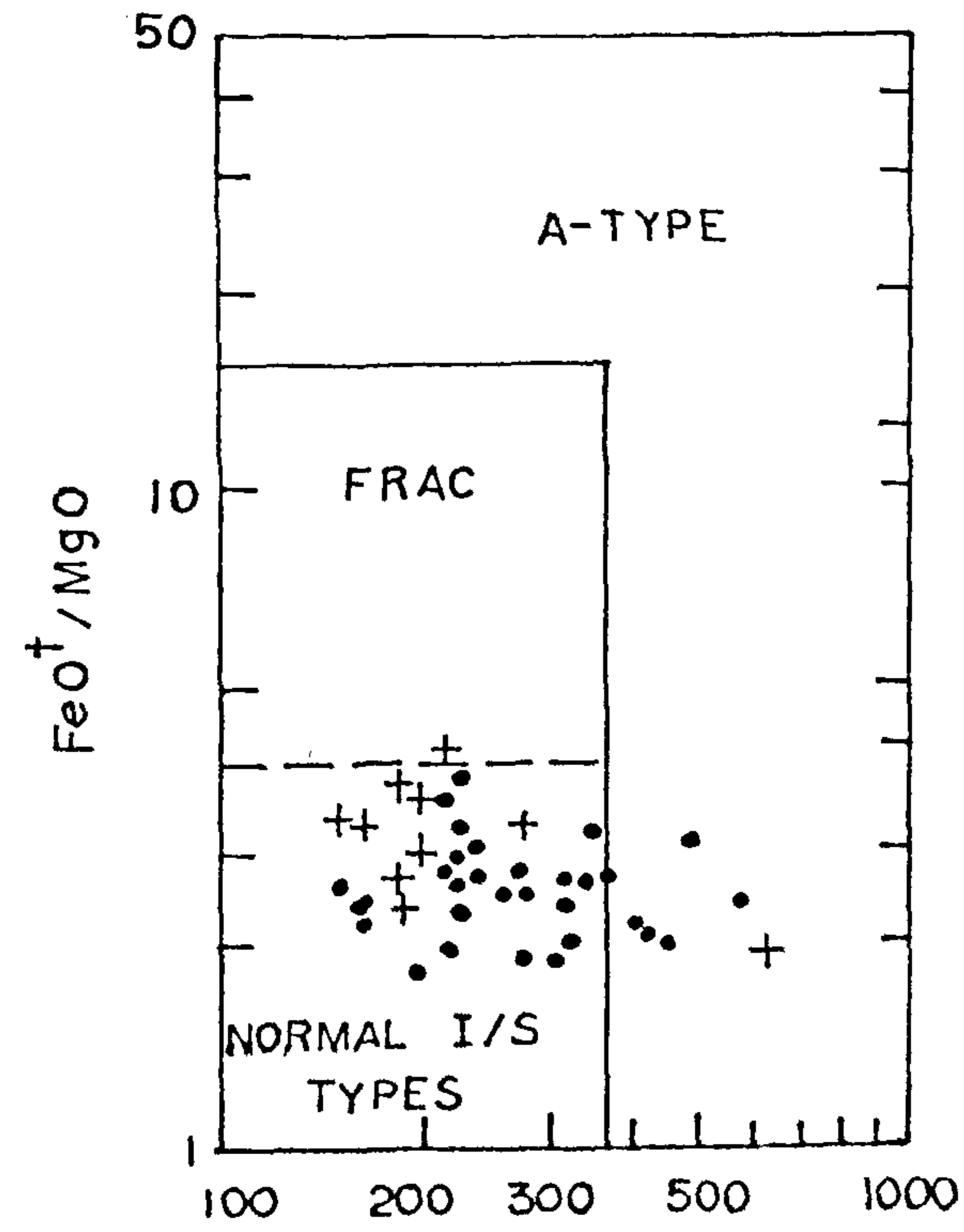
Figure 3. Na_2O vs K_2O diagram.Figure 4. Ba/Rb vs $(1/3 Si + K) - (Ca + Mg)$ variation diagram.Figure 5. Ba/Sr vs $(1/3 Si + K) - (Ca + Mg)$ variation diagram.

(10 cm–150 cm wide) of the leucocratic biotite-poor variant, seen in BRG and adjoining gneiss, have sharp discordant contacts. BPG is medium to fine-grained, generally equigranular and mineralogically similar to BRG except for low content of biotite. Biotite, the brown variety, is seen as disseminated specks. Both the granites fall in the syenogranite–monzogranite field in the Q–A–P diagram.

Pink feldspar pegmatite and aplite is the youngest phase consisting of narrow pegmatite and aplite dykes (1 cm to 20 cm wide), cutting across both BRG and BPG. The dykes chiefly comprise quartz and feldspar, the grain size varying from coarse to fine. Fluorite, molybdenite, pyrite and chalcopyrite mineralization is associated with this phase⁸.

The results of chemical analysis of 55 representative samples from different parts of the pluton are presented in Table 1. Major elements were determined following the methods of Vogel⁹ and Maxwell¹⁰ and trace elements in ICP–MS.

The variants of the granite, in general, show geochemical similarity. However, BRG contains more Na_2O , CaO , MgO , Fe_2O_3 , TiO_2 and P_2O_5 , while BPG has more SiO_2 , and Al_2O_3 . The typical major element characters of the granite are moderate to high silica, fairly high

Figure 6. $Zr + Nb + Ce + Y$ vs FeO^+/MgO diagram¹⁹.

K_2O and Na_2O , low MgO and CaO . The alkali content is comparable to that of the other granites of Kerala and elsewhere¹¹. Low CaO is as in calc-alkali granites¹². In Harker's variation diagram Al_2O_3 , CaO , MgO , Fe_2O_3 , TiO_2 and P_2O_5 define linear negative trends while the

other oxides remain more or less constant or show weak positive trends (Figure 2). K_2O and Na_2O values are higher than those suggested for granites¹³. A higher K-feldspar content, compared to plagioclase, is indicative of enrichment of K_2O over Na_2O and depletion of CaO with increase in silica. The higher content of Na_2O in BRG and K_2O in BPG, can be accounted by perthitization of K-feldspar and later metasomatism, respectively. Moderate to high content of Al_2O_3 has resulted in normative corundum in some cases, especially in BPG, indicating that alumina is in excess of calcium and alkalies. The alumina saturation index of Shand, using molar A/CNK values, which range between 0.89 and 1.12 (av. 0.98) for BRG and 0.97 and 1.10 (av. 1.06) for BPG, points to a weak peraluminous nature.

The Na_2O vs K_2O diagram¹⁴ (Figure 3) and CaO - Na_2O - K_2O diagram show granodiorite to adamellite composition of Kalpatta granite. In the AFM diagram, granite plots are in the calc-alkaline field, while they plot in the granite field in the An-Ab-Or normative diagram. Though I-type granites¹⁶ have A/CNK values less than unity, many are slightly peraluminous due to higher Al_2O_3 content. The low CaO , MgO , TiO_2 and high FeO'/MgO values of Kalpatta granite are similar to most A-type granites¹⁷⁻²¹. Silica-rich composition (generally $>68\% SiO_2$) is characteristic of many alkaline granite suites^{19,22}. The alkali content and Na_2O/K_2O ratio of the two variants of Kalpatta granite are as in A-type granites^{19,21}.

Trace elements like Cu, Zn, Cr, Co and Ni show inverse relationship with SiO_2 , whereas Pb, Th and U values increase with higher SiO_2 content in Kalpatta granite. The trace element content and distribution pattern are consistent with the empirical laws of fractionation.

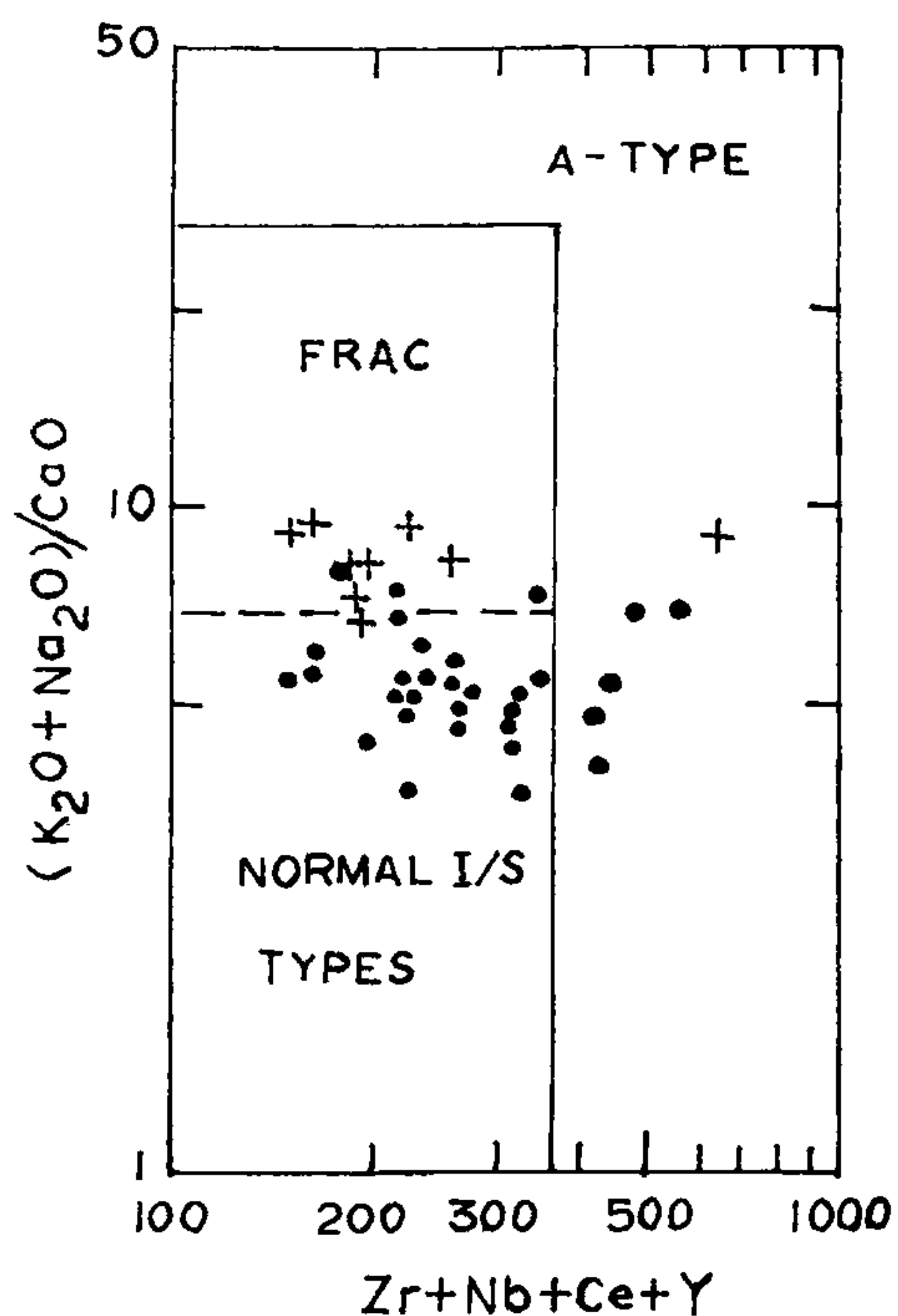


Figure 7. $Zr + Nb + Ce + Y$ vs $(K_2O + Na_2O)/CaO$ diagram¹⁹.

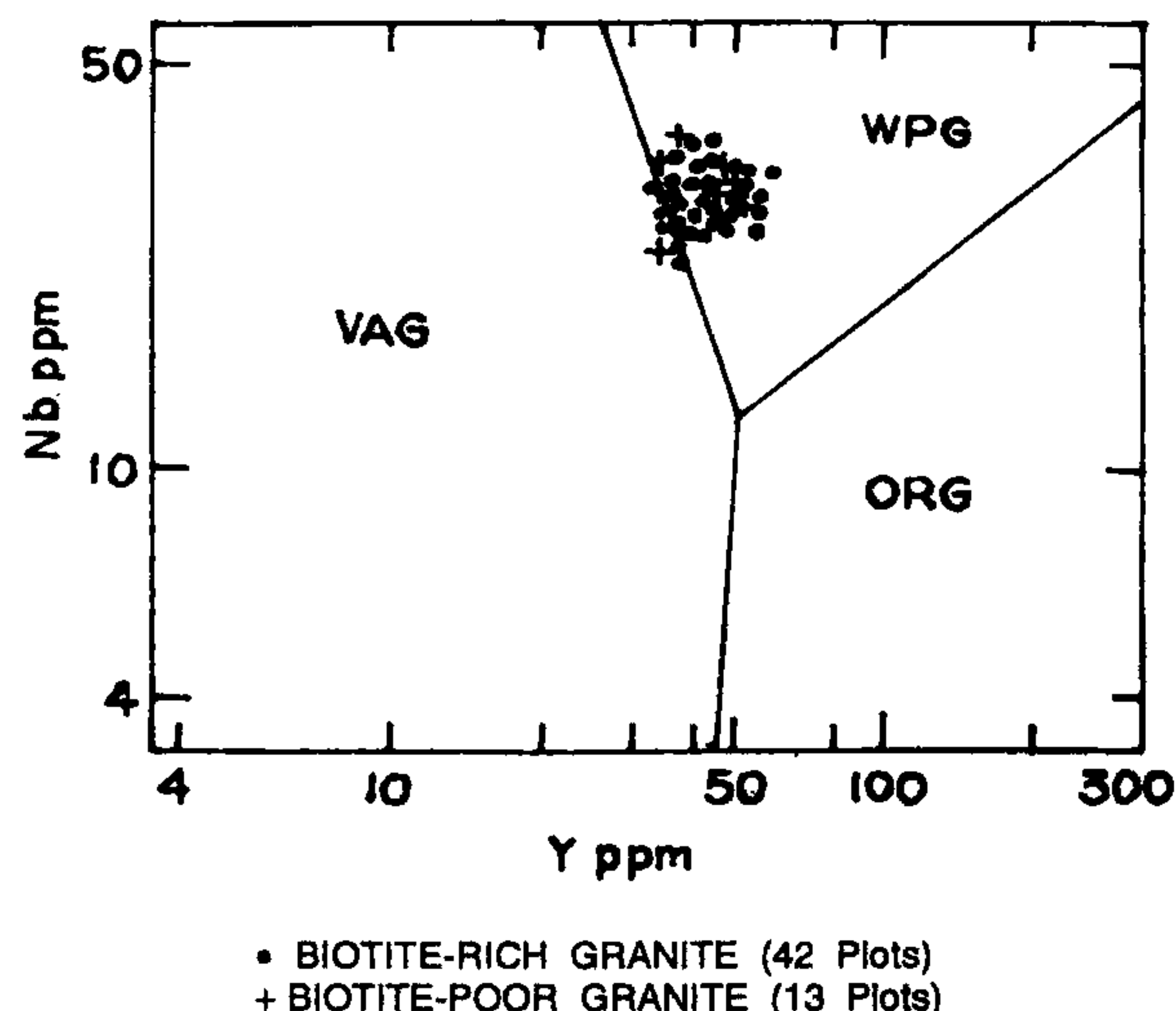


Figure 8. Y vs Nb plots of Kalpatta granite.

Trace element content of Kalpatta granite is similar to that of A-type granites¹⁹. Ba is high (389 to 1080 ppm) while Sr is comparatively low (80.21 to 198.99 ppm). Rb in the granite variants ranges from 60.45 to 136.15 ppm, giving a high K/Rb ratio (586 for BRG and 664 for BPG), which is characteristic of magmatic process¹⁹. The inverse relationship of Ba/Rb and Ba/Sr with (1/3 Si + K)–(Ca + Mg) is indicative of fractionation (Figures 4 and 5). The average Ba/Sr ratio for BRG and BPG is 5.61 and 5.01 respectively. During fractionation of feldspars, there is a drop in Ba/Sr ratio²³, which is clearly brought out in Figure 5. High Sr and low Rb content of the granite variants rules out a sedimentary parentage for the granite. Crustal participation in magma genesis could have lowered Y, Nb and Rb and increased the content of Al, resulting in both BRG and BPG falling in the transitional area between normal and fractionated granite (Figures 6 and 7).

Field and petrographic evidences clearly show the magmatic nature of Kalpatta granite variants. Major and trace element chemistry and geochemical classification schemes, supported by petrography, indicate close relationship among the different variants of the granite pluton. Mineralogical and geochemical signatures are characteristic of post-orogenic A-type granites. In the Y vs Nb discriminant diagram, most of the plots of Kalpatta granite fall in the within-plate granite field (Figure 8). Few plots outside this field could be due to crustal contamination leading to lowering of Nb and Y values. In Q-An-Or-Ab tetrahedral cotectic-eutectic, projection, where $P_{H_2O} = P_{total} = 5$ Kb on a eutectic surface of An-Ab-Or projected from quartz, the granite variants give a temperature of 650°C–685°C and a depth of emplacement of about 30 km on the basis of Rb-Sr values. Geochemical characters of Kalpatta granite are too tempting to suggest partial melting of the deeper parts of the crust, generating granitic magma, and its contamination during emplacement to higher crustal levels. The most probable mechanism of melting in stable interior is mantle upwarping producing rapid decompression melting resulting in anorogenic magmatism. Crustal distension can lead to extensive mantle degassing, resulting in the addition of volatiles producing localized melting^{22,24,25}. In such cases slightly peralkaline magma can be generated by partial melting of lower crust under a high flux of mantle-derived halogen-rich volatiles, which in turn explains the high concentration of alkalies and HFS elements in anorogenic granites²⁵. This model is applicable to Kalpatta granite as it has

high concentration of HFSE (e.g. Zr, 115.27 ppm–32.34 ppm; Nb 30.71 ppm–31.26 ppm). Presence of fluorapatite in both BRG and BPG and fluorite in late pegmatites of Kalpatta granite is characteristic of A-type granites, high F being the result of partial melting of F-rich biotite or amphibole. Thus the overall characters point to a magmatic source for Kalpatta granite pluton. The granite variants can be treated as products of polyphase late magmatic crystallization.

1. Thampi, P. K., Nair, P. K. R. and Balasubramonian, G., *Curr. Sci.*, 1993, **64**, 238.
2. Odam, A. L., Isotopic Age Determination of Rock and Mineral Samples from India, Final report, U.N. case 81-100084, 1982, unpublished, KMEDP, Trivandrum.
3. Nair, N. G. K., Soman, K., Santosh, M., Arkelyants, M. H. and Golubyev, V. N., *J. Geol. Soc. India*, 1985, **26**, 676.
4. Didier, J., in *Granites and their Enclaves*, Elsevier, Amsterdam, 1973, p. 393..
5. Pitcher, W. S., *The Nature and Origin of Granite*, Chapman and Hall, London, 1993.
6. Pitcher, W. S., in *Mountain Building Processes* (ed. Hsu, K.), Academic Press, London, 1983.
7. Maniar, P. D. and Piccoli, P. M., *Bull. Geol. Soc. Am.*, 1989, **101**, 635.
8. Kumar, S. N., Unpublished Ph D thesis, University of Kerala, Trivandrum, 1995.
9. Vogel, A. I., *Textbook of Quantitative Inorganic Analysis, Including Elementry Instrument Analysis*, E.L.B.S., 1978.
10. Maxwell, J. A., *Rock and Mineral Analysis*, Wiley, New York, 1968.
11. Rogers, J. J. W. and Greenberg, J. K., *J. Geol.*, 1990, **98**, 6.
12. Nockolds, S. R., *Bull. Geol. Soc. Am.*, 1954, **65**, 91.
13. Rogers, J. J. W. and Adams, J. A. S., in *Handbook of Geochemistry* (ed. Wedephol, K. H.), Springer Verlag, 1969, vol. 2, p. 5.
14. Harpum, J. R., *Rec. Geol. Surv. Tanganyika*, 1963, **10**, 80.
15. Kerr, A., *Precambr. Res.*, 1989, **45**, 1.
16. Chappel, B. W. and White, A. J. R., *Pac. Geol.*, 1974, **8**, 173.
17. Loiselle, M. C. and Wones, D. R., *Geol. Soc. Am.*, 1979, **174**, 225.
18. White, A. J. R. and Chappel, B. W., *Geol. Soc. Am.*, 1983, **159**, 21.
19. Whalen, J. B., Currie, K. L. and Chappel, B. W., *Contrib. Mineral. Petrol.*, 1987, **95**, 407.
20. Anderson, J. L. and Bender, E. E., *Lithos*, 1989, **23**, 19.
21. Tack, L., Liegeois, J. P., Deblond, A. and Duchesne, J. C., *Precambr. Res.*, 1994, **68**, 323.
22. Sylvester, P. J., *J. Geol.*, 1989, **97**, 261.
23. Heir, K. S. and Taylor, S. R., *Geochim. Cosmochim. Acta*, 1959, **17**, 286.
24. Bailey, D. K., in *The Alkaline Rocks*, John Wiley, New York, 1974.
25. Harris, N. B. W. and Marriner, G. F., *Lithos*, 1980, **13**, 325.

Received 14 February 1997; revised accepted 21 January 1998